JOURNAL OF AMERICAN MEDICAL SCIENCE & RESEARCH

Original Research Article
ISSN: 3041-5578
Journal homepage: https://medical.researchfloor.org/

Synthesis and Characterization of Gold Nanoparticles (AuNPs) from *Chrozophora rottleri* (Geiseler) Spreng. An Evaluation of Antioxidant and Antimicrobial Activities

K. Hymavathi and A. Sabitha Rani

Department of Botany, University College of Science, Osmania University, Hyderabad, Telangana, -500 007 India

ABSTRACT

This is the first report of its kind on the study. Applications for nanobiotechnology include coatings, cosmetics, packaging, biomedicine, and boosting biological activity. Given the importance of Chrozophora rottleri (Euphorbiaceae) we developed gold nanoparticles (AuNPs) economically and ecologically responsibly. In less than a minute, the color of the gold nanoparticles (AuNPs) synthesized in this work changed from yellow to wine red. Advanced methods such as UV-visible spectroscopy, Fourier transform infrared (FT-IR), scanning electron microscopy (SEM), X-ray diffraction (XRD), and zeta potential (ZP) were used to study these nanoparticles. The synthesized gold nanoparticles' anti-microbial (bacterial and fungal) and in vitro antioxidant (DPPH and H2O2) characteristics were evaluated. Standard ascorbic acid concentrations of 10, 25, 50, 75, and 100 µg/ml were used to investigate the DPPH free radical scavenging activity. The findings showed that 18.53±0.162 was the lowest percentage of inhibition and 83.62±0.785 was the greatest. Analogously, the ascorbic acid hydrogen peroxide radical scavenging (H_2O_2) assay revealed that the maximum % inhibition was 87.27±0.467 and the lowest was 19.52±0.225. The Agar well-diffusion method was used to examine the antibacterial effectiveness of ampicillin and synthesized gold nanoparticles (AuNPs). Four distinct concentrations (25, 50, 75, and 100 µl) were assessed in relation to several bacterial pathogens, such as Escherichia coli, Streptococcus pneumoniae, Pseudomonas aeruginosa, and Staphylococcus aureus. Elevated doses of traditional Ampicillin demonstrated a progressive degree of inhibitory impact on E. coli and S. aureus, signifying heightened antimicrobial efficacy. Zones measuring 16 mm, 20 mm, 22 mm, and 25 mm were seen in ampicillin, while zones measuring 11 mm, 13 mm, 14 mm, and 16 mm were seen in E. coli The synthesized gold nanoparticles (CR-AuNPs) demonstrated increased zones of inhibition measuring 1.2 mm, 12 mm, 14 mm, and 17 mm, indicating greater antibacterial activity against S. pneumoniae. Similar to this, P. aeruginosa was inhibited by AuNPs, and the zones of inhibition measured 0.6 mm, 12 mm, 16 mm, and 18 mm. The CR-AuNPs show activity against S. aureus, E. coli, S. pneumoniae, and P. aeruginosa at a concentration of 200 µg/ml, which is the minimum inhibitory concentration (5, 10, 25, 50, 100, and 200 µg/ml). The well diffusion method was utilized to evaluate the antifungal efficacy of AuNPs and Fluconazole against Aspergillus niger. The findings showed that the zones of inhibition, which measured 12 mm, 16 mm, 21 mm, and 25 mm, gradually increased. Moreover, the zones of inhibition against Candida albicans were observed to be 13 mm, 16 mm, 18 mm, and 22 mm. At 12 mm, 15 mm, 19 mm, and 23 mm, the CR-AuNPs showed increasingly wider zones of inhibition against Aspergillus niger. Furthermore, 11 mm, 14 mm, 17 mm, and 19 mm zones of inhibition were seen in Candida albicans. The findings point to the potential for producing gold nanoparticles (AuNPs) using green synthesis methods that are both economical and ecologically benign. Moreover, this work is the first to suggest that C. rottleri may have antioxidant and antibacterial properties. As a result, this creates new chances in various fields in addition to medicines.

Citation: K. Hymavathi and A. Sabitha Rani (2024). Synthesis and Characterization of Gold Nanoparticles (AuNPs) from *Chrozophora rottleri* (Geiseler) Spreng. An Evaluation of Antioxidant and Antimicrobial Activities. *Journal of American Medical Science and Research.*

DOI: https://doi.org/10.51470/AMSR.2024.03.02.01

Received on: 15 May, 2024
Revised on: 08 June, 2024
Accepted on: 13 July, 2024

Corresponding Author: ***K. Hymavathi***
Email Address: ***hyma.kukudala@gmail.com***

Keywords: *AuNPs, synthesis, anti-microbial, antioxidant, Chrozophora rottleri, and Euphorbiaceae*

Introduction

Nanotechnology, the science of manipulating materials at the scale of 10–1000 nanometers, has emerged as a transformative field that intersects engineering, biology, chemistry, and physics [1-2]. This multidisciplinary approach leverages the unique properties of nanoparticles—such as their size, optoelectronic characteristics, and structural morphology—to drive innovations across diverse applications, particularly in biomedical and food sciences [3-4]. In recent years, the quest for sustainable and eco-friendly methods of nanoparticle production has gained momentum, leading to the development of green synthesis techniques. Green synthesis offers an environmentally conscious alternative to conventional methods by utilizing biological materials to reduce metal salts to nanoparticles. This approach not only facilitates the production of nanoparticles but also stabilizes them through the formation of a "biological corona," which enhances their biocompatibility and affects their functional properties [5]. The green synthesis of nanoparticles is particularly promising due to its cost-effectiveness, reduced toxicity, and minimal environmental impact, making it a viable option for large-scale applications [6]. Nanoparticle synthesis can be achieved through two primary approaches: top-down and bottom-up methods. The bottom-up approach, which builds nanoparticles from simpler molecules, is particularly favored for its efficiency and scalability. Plant-based green synthesis methods are especially advantageous due to their simplicity and cost-effectiveness compared to microbial methods [7-9]. Among various metallic nanoparticles, gold nanoparticles (AuNPs) have garnered significant attention due

to their unique properties and broad range of applications. Gold, traditionally known for its inertness and biocompatibility, has found new relevance in nanotechnology. The physical and chemical properties of gold nanoparticles, including their small size (1–100 nm), optical characteristics, and ease of fabrication, make them ideal candidates for applications in cancer therapy, drug delivery, food safety, water treatment, and beyond [10-12]. Their exceptional robustness, targeted binding capabilities, and varied shapes further enhance their utility across diverse fields [13]. the transformative potential of nanotechnology and green synthesis, particularly focusing on the promising applications and properties of gold nanoparticles, setting the stage for further exploration and innovation in this dynamic field.

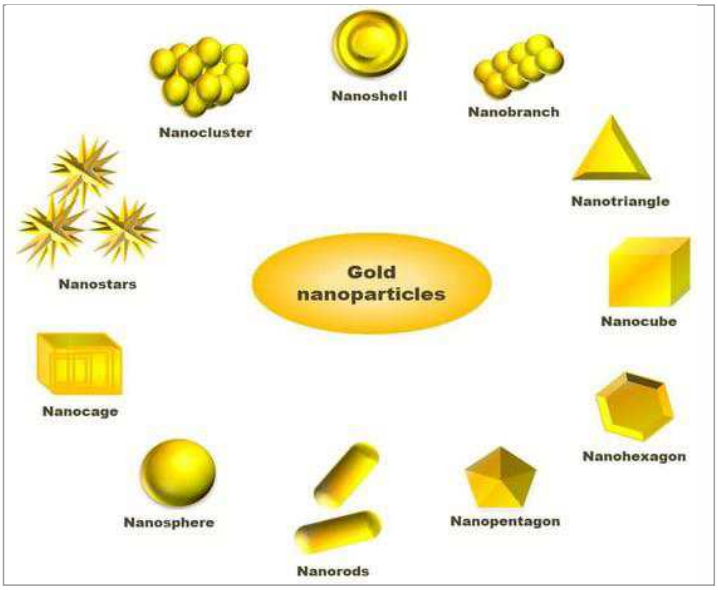

Fig: 1. Different shapes available for gold nanoparticles.

Gold nanoparticles (AuNPs) have gained considerable prominence in the medical and scientific communities due to their versatile applications and distinctive properties. Historically, gold's medicinal potential was noted as early as 1890 by Robert Koch, who observed the antibacterial effects of gold compounds against tuberculosis bacilli [14]. This early recognition paved the way for the development of gold nanoparticles, which were first systematically studied by Michael Faraday in 1857. Faraday's research on the optical properties of colloidal gold laid the foundation for understanding its unique light-scattering behavior [15]. In contemporary science, AuNPs are renowned for their wide-ranging applications in diagnostics, sensor development, photo imaging, and photothermal therapy [16-17]. The antibacterial properties of AuNPs, which involve mechanisms such as disruption of bacterial cell walls and inhibition of DNA replication, have led to their exploration as alternatives or complements to conventional antibiotics [18]. This makes AuNPs promising candidates for addressing the challenges posed by multidrug-resistant pathogens.

The appeal of AuNPs extends beyond their antibacterial potential. Their non-toxic nature, combined with their high absorbance and unique electronic and optical properties, has driven their use in various health-related applications [19-20]. Research has demonstrated that AuNPs are effective in biosensor technology, cancer cell destruction, and as antioxidant agents [21-22]. Their intrinsic redox activity and stability make them suitable for applications requiring radical trapping, superoxide dismutase-like, and catalase-like activities [23-24].

Among the various synthesis methods, green synthesis has emerged as a sustainable and eco-friendly approach for producing AuNPs. This method, utilizing plant extracts or other biological materials, offers an effective means of generating nanoparticles with antimicrobial, anticancer, anti-inflammatory, antioxidant, and immunomodulatory properties [25]. The green synthesis of AuNPs not only ensures biocompatibility and low cytotoxicity but also enhances their potential for therapeutic and diagnostic applications [26-27].

Gold nanoparticles synthesized through green technologies are being explored for their catalytic properties in environmental and analytical applications. They are employed in the decomposition of pollutants, detection of contaminants in various matrices, and as electrode modifiers for enhancing analytical sensitivity [28-31]. One plant of interest in green nanoparticle synthesis is *Chrozophora rottleri* (Geiseler) Spreng., commonly known as *Suryavarti*. This plant, native to regions including India, Myanmar, and Thailand, has been traditionally used in medicine for a variety of ailments. Its applications range from wound healing and treatment of respiratory conditions to purgative and dyeing purposes [32-35]. Recent studies highlight its potential in phytotoxic and anti-helmintic activities, underscoring its value as a source for nanoparticle synthesis [36-37]. The integration of gold nanoparticles into medical and environmental applications showcases their multifaceted utility and underscores the importance of sustainable synthesis methods in advancing their use.

Pharmalogical activities of *Chrozophora rottleri*

Antioxidant activity [39-39] Anti-bacterial [40-42] Anthelmintic- [43] Anti-fungal [44], Anti-diabetic [45].

Material and Methods

Collection and Authentication of Plant Material

About 500 gr of the plant material *C. rottleri* was collected from the Udimilla Village (16.46454 Latitude and 78.96125 Longitude), Amrabad Tiger Reserve (Nallamala Hills Nagarkurnool District, in the Telangana state of India, based on its medicinal properties and ease of availability, during July / August in the year 2023. The plant was taxonomically identified and authenticated by Botanical Survey of India, Deccan Regional Centre, Hyderabad, Telangana (accession number-BSI/DRC/2023-24/Identification/733), and the specimen was preserved at Herbarium, Hyderabadensis, Department of Botany, O.U, Hyderabad, Telangana, India.

Preparation of *C. rottleri* aqueous leaf extract

The leaves were shed-dried for approximately 8–10 days after being collected and properly cleaned with tap water to eliminate dirt, then again with distilled water (DW). When the leaves had dried, they were all blended into a fine powder with an electric blender (LG, India) and kept for later use at room temperature in an airtight container with a label. A magnetic stirrer (REMI, India) was used to boil 10 grams of the fine powder with 100 milliliters of water to produce a 10% aqueous leaf extract, which was then left to steep for 60 minutes at 60 degrees Celsius. Following its filtration via Whatman filter paper no. 1, the crude extract was kept in a refrigerator (LG, India) at a temperature between at 2–4 °C.

Synthesis of Gold Nanoparticles (AuNPs) of *C. rottleri*

Singh *et al.,* (2022), employed a previously documented process for the manufacture of the nanoparticles.

The pH of the resulting Au-NPs was subsequently adjusted to 5 and 10, respectively. After being combined with 10 ml of a 10 mM $HAuCl_4$. $3H_2O$ solution at room temperature, 125 µl of plant extract (60g/100 ml H_2O) was heated for 30 minutes at 70 °C gradually while constantly whisking. The shift in hue and it was noted that the gold solution's yellow hue quickly changed to a wine-red hue, indicating that the synthesis of AuNPs had been confirmed. In this case, the leaf extract quickens the production of AuNPs while reducing the gold ions. The bottom-up approach's mechanism was followed during the preparatory phase. the conversion of $3H_2O$ + $HAuCl_4.3H_2O$ to AuNPs. Additionally, the produced AuNPs were collected by centrifugation at 2000 rpm for 20 minutes, dried at 70 °C in a hot air oven, and kept for later use in a plastic sample vial labeled appropriately.

Characterization of AuNPs of *C. rottleri*

The green-synthesized nanoparticles were characterized using a range of analytical techniques to confirm their formation and stability. UV–visible spectrophotometry was employed to monitor the absorption peaks between 350 and 800 nm, revealing information about the nanoparticles' size and surface plasmon resonance. Fourier Transform Infrared Spectroscopy (FT-IR) with a Perkin-Elmer instrument was used to identify functional groups and confirm the presence of stabilizing agents on the nanoparticles. X-ray diffraction (XRD) analysis, conducted with a Philips PW 1830 instrument, provided insights into the crystalline structure and phase of the nanoparticles. Additionally, particle size and zeta potential were measured using a Malvern Zetasizer NanoSizer to determine the size distribution and stability of the nanoparticle dispersions. These techniques collectively ensured a thorough characterization of the nanoparticles, validating their suitability for various applications.

Ultraviolet–visible spectroscopy analysis

UV spectrometry was used for gold nanoparticles confirmation. At 25 to 280C, same volume of samples (0.5mL) were examined. The spectra of gold nanoparticles in aqueous solution, analyzed between 340 and 800 nm, were used to evaluate the progress of the reaction between metal ions and the leaf extract [45-46].

Fourier Transforms Infrared Spectroscopy (FTIR)

The gold NP solution was centrifuged for 30 minutes at 10,000 rpm. Three or four thorough washes of the supernatant solution were conducted in order to eliminate any unbound proteins or enzymes that are not capping the gold NPs. A vacuum drier was used to dry the pellet.

A dry leaf powder of *C. rottleri* was obtained and measured at a resolution of 4 cm-1 utilizing the diffuse reflection mode of the potassium bromide (KBr) pellet technique in Fourier transform infrared (FTIR, CFRD, Osmania University, Hyderabad, Telangana) spectroscopy. An infrared light with a wavelength of 500–4000 cm−1 was used to mix the powder with KBr. For the FTIR analyses of *C. rottleri* extract prior to and following bio reduction, a comparable procedure was employed [47-48]. The force constant and reduced mass are the two factors that determine the frequency of the vibrational peak (ν), and these factors can be expressed by the following equation.

$$\nu = 1/2\pi c \sqrt{(k/\mu)}$$

Here, c- is the speed of light,
k- is the force constant
µ- is the reduced mass **X-Ray diffraction**

X-Ray Diffraction (XRD) was performed using a Bruker D8 Advance LYNXEYE XE-T system at CSIR-IICT, Hyderabad, Telangana, operating at 40 mA and 40 kV with CuKα radiation. The analysis was conducted at various 2θ angles to determine the size, crystalline structure, and chemical composition of the purified gold nanoparticles (AuNPs). The mean size of the AuNPs was calculated using the Scherrer equation, as described by [49].

The mean diameter of the nanoparticles (D, in nm) was calculated using the Scherrer equation:

$$D = \frac{K\lambda}{\beta \cos\theta}$$

Where λ is the wavelength of the X-ray source (0.15406 nm), \ (K\) is the Scherrer constant (0.9), βis the angular width at full width at half maximum (FWHM) of the diffraction peak, and θ is the Bragg's diffraction angle.

Scanning Electron Microscopy

The silver nanoparticles pellet was analyzed using Scanning Electron Microscopy (SEM). To prepare the sample, a thin film was formed on a carbon-coated copper grid by applying a small drop of the nanoparticle solution. The excess solution was gently removed with blotting paper, and the film was left to dry thoroughly before SEM examination. This preparation method ensured clear imaging of the nanoparticle morphology and distribution.

Zeta sizer and zeta potential

The stability and surface charge of the gold nanoparticles (AuNPs) were assessed using zeta potential analysis. The measurements were conducted with a Malvern Zetasizer Nano ZS, equipped with a laser Doppler system. Deionized water was used to dilute the nanoparticles, minimizing scattering effects. The sample was analyzed over a calibrated area of 2 mm, with a count rate of 101.9 kilo counts per second (kcps) over a duration of 60 seconds, as described by [50].

DPPH Free Radical Scavenging Activity

The free radical scavenging activity of the synthesized gold nanoparticles (AuNPs) from C. rottleri was evaluated using the 1,1-diphenyl-2-picryl hydrazyl (DPPH) method, following the protocols outlined by [51]. This assay measures the reduction of DPPH, a stable free radical, in methanol solution in the presence of hydrogen-donating antioxidants. The reduction of DPPH results in a color change from purple to yellow.

For the analysis, varying concentrations of AuNPs (10, 25, 50, 75, and 100 µg/ml) were prepared in 1 ml of a 0.2 mM DPPH methanol solution. The DPPH solution was freshly prepared, and its optical density (OD) was adjusted to 0.8; if necessary, additional DPPH or methanol was added to achieve this OD. The mixture was thoroughly mixed and incubated for 30 minutes. The optical density of the resulting solution was then measured at 517 nm using a Hitachi 2010 spectrophotometer. The percent inhibition of antioxidant activity was calculated using the formula:

Percentage of inhibition= (Control OD−Test OD)/ Control OD/×100

The readings of the test samples were compared with those of the positive control, ascorbic acid (Vitamin C).

Hydrogen peroxide radical scavenging (H_2O_2) Assay

The hydrogen peroxide radical scavenging assay (SA) of synthesized (AuNPs) of *C. rottleri*, was tested by following the procedure suggested by [52]. Hydrozen peroxide solution 40mM was prepared in phosphate buffer (1M pH 7.4), and the hydrogen peroxide concentration was determined by absorption at 230nm by using a spectrophotometer. CR Gold nanoparticles of varying concentration (10-100 µg/ml) in distilled water were added to hydrogen peroxide, and the absorbance at 230nm was determined after 10 min against a blank solution containing phosphate buffer without hydrogen peroxide. The percentage of hydrogen peroxide scavenging was calculated as follows:

% scavenging activity SA = $[A_{control} - A_{sample}] / A_{control} \times 100$

Where $A_{control}$ is the absorbance of the control and A_{sample} is the absorbance of the test sample. The experiments were run in triplicates.

Antimicrobial activity of *C. rottleri*

Synthesized Au nanoparticles were tested for antibacterial efficacy against various types of bacteria's and fungus, which served as test microorganisms.

Antibacterial activity

Bacterial Strains:

The bacterial strains used in the study, including Gram-positive *Staphylococcus aureus* (ATCC 25923), *Streptococcus pneumoniae* (ATCC 33400), and Gram-negative *Pseudomonas aeruginosa* (ATCC 27853) and *Escherichia coli* (ATCC 25922), were obtained from the American Type Culture Collection (ATCC).

Media Preparation for Anti-Bacterial Activity:

A) Nutrient Agar Media

Nutrient Agar was commercially procured, and 28.0 grams of the powder were dissolved in 1000 ml of distilled water, mixing thoroughly. The nutrient agar solution was then sterilized in an autoclave at 121°C for 15 minutes. Once sterilized, the media was used for preparing plates to study the antibacterial activity.

B) Nutrient Broth

Nutrient Broth was procured commercially, and 1.3 grams of the powder were dissolved in 100 ml of distilled water, mixing thoroughly. The nutrient broth solution was then sterilized in an autoclave at 121°C for 15 minutes. After sterilization, the broth was used for preparing the bacterial inoculum.

C) Preparation of stock solution

Stock cultures for each bacterial organism were prepared by aseptically sub-culturing the confirmed test organisms onto two nutrient agar slants. One slant was maintained as the stock culture, while the other was used as the working culture. These bacterial cultures were stored at 4°C for short-term use. Additionally, a glycerol stock of each organism was preserved at -20°C for long-term storage.

D) Inoculum preparation

The bacterial pathogens were inoculated into nutrient broth and incubated at 37°C for 24 hours. The resulting cultures were then adjusted to a concentration of approximately 10^5 CFU/ml.

Antibacterial activity

The antibacterial activity of the synthesized gold nanoparticles (AuNPs) from C. rottleri was assessed using the Agar well-diffusion method. Four concentrations of AuNPs (25, 50, 75, and 100 µl) were tested against bacterial pathogens including *Staphylococcus aureus, Streptococcus pneumoniae, Pseudomonas aeruginosa*, and *Escherichia coli*. The plates were incubated at 37°C for 18-24 hours. After incubation, the diameter of the inhibition zones (in mm) was measured, and the activity index was calculated. Measurements were taken in three different fixed directions on each plate, and the average values were recorded, following the protocols outlined by [53].

Minimum Inhibitory Concentration (MIC)

The Minimum Inhibitory Concentration (MIC) is defined as the lowest concentration of an antimicrobial agent that inhibits the visible growth of a microorganism after overnight incubation [54].

Compound Preparation

Compounds were weighed individually to 1 mg each and dissolved in methanol to achieve a final stock concentration of 1 mg/ml. A standard solution of ampicillin was prepared using the same method for comparative analysis.

Culture Preparation

A loopful of culture was inoculated into 3 ml of nutrient broth and incubated at 37°C overnight in a shaking incubator.

Inoculum Preparation

From the overnight-grown culture, 20 µl was inoculated into 1.5 ml of nutrient broth. Different concentrations of the compound were added, and the mixture was incubated at 37°C overnight in an incubator.

Result

After 24 hours of compound treatment, the tubes were observed, and the results were recorded.

Anti-Fungal Activity

Fungal Strains

The fungal strains *Candida albicans* (MTCC 183) and *Aspergillus niger* (MTCC 281) used in the study were obtained from the Microbial Type Culture Collection (MTCC) at the Institute of Microbial Technology (IMTECH), India

Sabouraud Dextrose Agar (SDA):

Sabouraud Dextrose Agar (SDA) was procured commercially. To prepare the medium, 32.5 grams of the powder were dissolved in 500 ml of distilled water and mixed thoroughly. The solution was then sterilized in an autoclave at 121°C for 15 minutes. Once sterilized, the SDA was used to prepare plates for evaluating antifungal activity.

Antifungal activity

The antifungal activity of synthesized gold nanoparticles (AuNPs) from *C. rottleri* was tested using the well diffusion method. SDA culture plates were inoculated with *Candida albicans* and *Aspergillus niger* using the spread plate technique. The plates were then incubated at 37±2°C for 48 hours. After incubation, the plates were examined for zones of inhibition around the wells, and the diameter of these zones (in mm) was measured [55].

Results

Table: 1. Taxonomical features of Chrozophora rottleri (Geiseler) A.Juss. ex Spreng

Kingdom	Plantae
Phylum	Streptophyta
Class	Equisetopsida
Sub class	Magnoliidae
Order	Malpighiales
Family	Euphorbiaceae
Genus	*Chrozophora*
Species	*Chrozophora rottleri*

Habit: Herb

Habitat/Ecology

Chrozophora rottleri is mainly distributed in India, Myanmar, Thailand, Andaman Islands, and Malaysia. It commonly grown in wet places like waste areas, along roads, and along and in stream beds. Soil: clay (mud), sand.

Description

Chrozophora rottleri belongs to the Euphorbiaceae family and is commonly known as Suryavarti. In Telugu, it is referred to as "Erra miriyamu" or "Linga mirapa." This herbaceous plant is characterized by its erect growth with silvery hairs. The lower part of the stem is bare, while the upper part is hairy. It features a slender taproot and can grow up to 75 cm tall. The plant has ascending branches that are trichotomously forked from the base. The leaves are alternate, broadly ovate, measuring 2–6 × 1.5–7 cm, and are (sub) coriaceous with three nerves from the base. The veins are deeply impressed, and the petiole can be up to 8 cm long, with two glands at the base of the lamina. The inflorescence is a terminal raceme, tomentose, up to 3 cm long. Male flowers are (sub) sessile, crowded in the upper axils, with yellow stamens, while female flowers are pedicellate and positioned below.

The tepals are arranged in two series of 5 + 5, with the inner ones being petaloid. There are 12–15 stamens in two series, which are connate, with the inner stamens being longer. The ovary is 3-locular with three axile ovules and three red, bifurcate styles. There are five disc glands. The capsule is depressed, 3-lobed, stellate tomentose, and 0.8 cm across. The fruit is a capsule with globose seeds (Fig. 1).

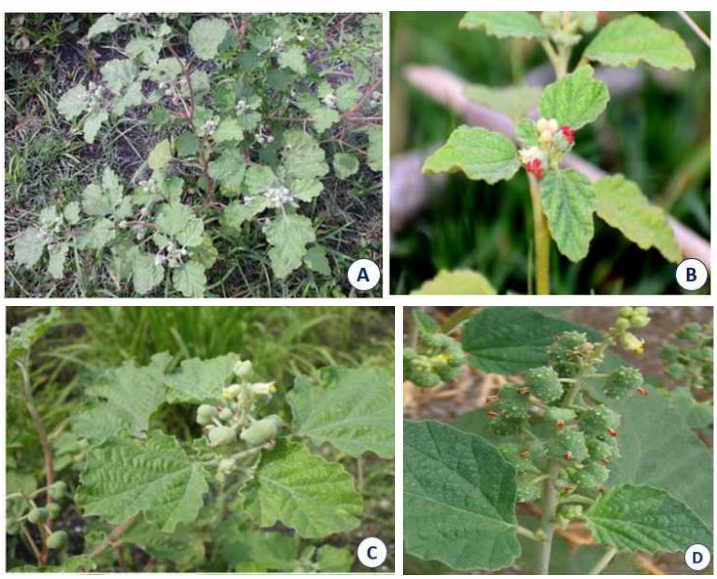

Fig. 2A-F: C. rottleri habitat

Synthesis of Gold (AuNPs) Nanoparticles from *C. rottleri*

125 µl of the plant extract (60 g/100 ml H_2O) was mixed with 10 ml of a 10 mM $HAuCl_4 \cdot 3H_2O$ solution at room temperature. The yellow-colored gold solution turned to a wine red color within a minute, indicating the synthesis of gold nanoparticles (AuNPs). The synthesized AuNPs were then characterized and stored at 4°C until further experiments (Fig. 3).

Fig: 3. Schematic representation of the synthesis of CR-AuNPs

Characterization of Gold nanoparticles (AuNPs) from *C. rottleri*

Synthesized gold nanoparticles of *C. rottleri* were characterized by Fourier-Transform Infrared Spectroscopy (FTIR). UV Spectroscopy (UV-Vis), Scanning Electron Microscope (SEM), X-ray powder diffraction (XRD), and Zeta potential (ZP).

Fourier-Transform Infrared Spectroscopy (FTIR)

Fourier transform infrared spectroscopy (FT-IR) is used to study the bio-reduction compounds responsible for the creation of gold nanoparticles (AuNPs) by *C. rottleri*. The FT-IR spectra of *C. rottleri*- AuNPs exhibited absorption peaks at certain wavenumbers: 692.47, 1641.78, 1631.83, 1901.88, 2370.59, 2931.90, 2931.90, 3419.90, and 3522.13 cm-1. Ten scans were performed for each sample to get the FT-IR spectra. The spectra were obtained with a resolution of four cm-1 and covered a range from four thousand to four thousand cm-1. The observed peak at 692.47 is attributed to the =C-H Alkane. The detected peaks at 1631.83 and 1641.78 correspond to the C-O Alkenyl. The peak at 1901.88 is linked to the presence of C=CH aliphatic compounds, while the peak at 2370.59 is associated with the presence of C=C alkynes. The carboxylic acid is shown by the peak at 2931.90, whilst the amides C=N-H and N-H amine and amides are indicated by the peaks at 3419.90 and 3522.13, respectively **(Fig: 4).**

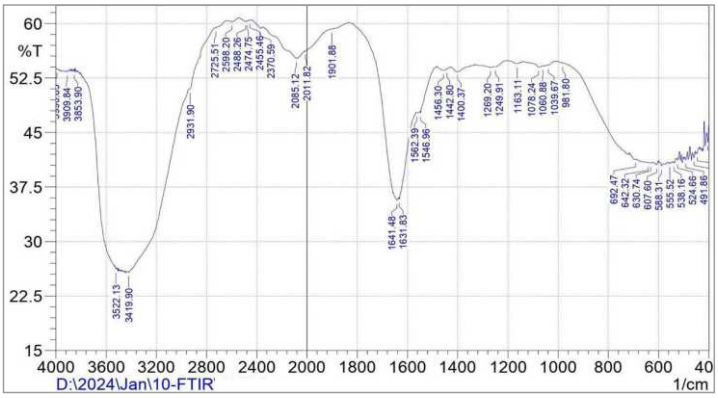

Fig: 4. FTIR spectral image of CR-AuNPs

UV-Visible spectroscopy (UV-Vis)

The synthesized gold nanoparticles (AuNPs) of *Chrozophora rottleri,* have been confirmed by UV spectrometry, a method that gauges the light-absorbing capacity of the particles at different wavelengths. These gold nanoparticles' spectra were examined between 340 and 800 nm, which is a key wavelength for recognizing the distinctive surface plasmon resonance (SPR) peaks of these particles. The size, shape, and mode of the nanoparticles' creation are all indicated by these SPR peaks.

The spectrometric analysis of *C. rottleri* leaf extract revealed (580nm and 620 nm) the optimal conditions for producing gold nanoparticles, with phytochemicals serving as stabilizing and reducing agents. The successful creation and stability of gold nanoparticles were confirmed by specific absorbance peaks, indicating strong interaction between metal ions and bioactive chemicals.

All things considered, the UV-Vis spectrometric analysis played a crucial role in characterizing the produced gold nanoparticles by offering a thorough grasp of their optical characteristics and the fundamental processes that led to their creation using the *C. rottleri* leaf extract **(Fig:5).**

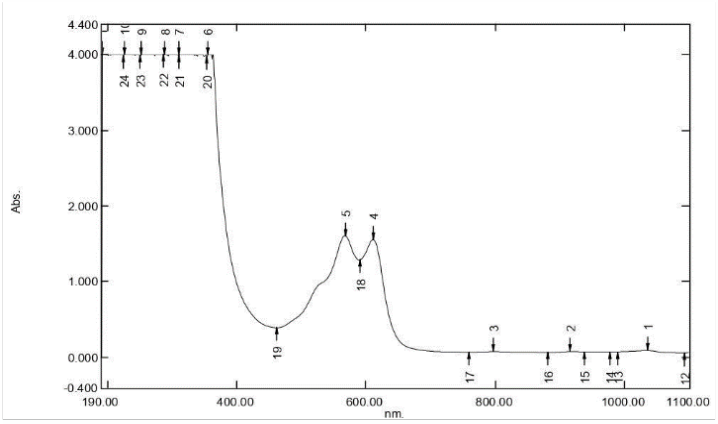

Fig: 5. UV-Visible spectroscopy (UV-Vis) CR-AuNPs

Scanning Electron Microscope (SEM)

A scanning electron microscope (SEM) is a type of electron microscope that provides detailed images of the surfaces of various entities, allowing for precise examination of their dimensions and shape. SEMs operate by scanning a focused beam of electrons across the sample's surface. The interactions between the electrons and the atoms on the surface generate signals that are used to construct high-resolution images, revealing the surface topography and composition.

In this study, a detailed examination of the size and shape of gold nanoparticles synthesized using *Chrozophora rottleri* (CR-AuNPs) was conducted using a Hitachi 500 scanning electron microscope. The SEM was operated at an accelerating voltage of 15.0 kV and a magnification of 100.00 µm. These settings allowed for a clear visualization of the nanoparticles, ensuring accurate measurement of their morphological characteristics.

The SEM images revealed that the CR-AuNPs predominantly exhibit a round shape, with diameters ranging from 132 to 146 nm. This consistent round morphology indicates a uniform synthesis process facilitated by the *C. rottleri* extract. The size distribution within this narrow range suggests that the phytochemicals in the CR extract effectively controlled the nucleation and growth phases of the nanoparticle synthesis, leading to the formation of nanoparticles with relatively uniform dimensions.

The use of SEM in this analysis provided a comprehensive and detailed assessment of the CR-AuNPs, confirming their successful synthesis and characterizing their morphological properties. This information is vital for further optimizing the synthesis process and exploring the functional applications of these gold nanoparticles **(Fig:6).**

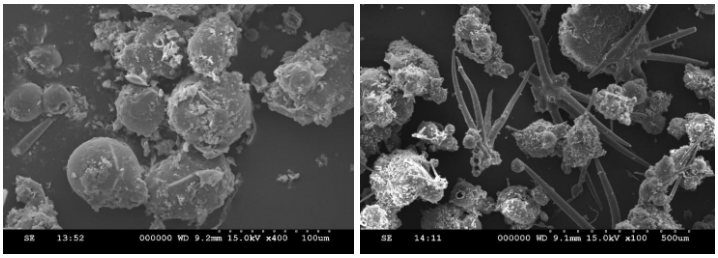

Fig:6. SEM image of CR-AuNPs

XRD Spectra of AuNPs

X-ray diffraction (X-RD) was employed to ascertain the crystal structure and dimensions of nanoparticles. The peaks seen at 38.157, 44.287, 64.643, and 77.689 degrees correspond to the facets of the face-centered cubic (fee) structure of gold nanoparticles (AuNPs) derived from *C. rottleri* leaf extract. The reflections correspond to the crystallographic planes with Miller indices (111), (200), (220), and (311). In addition, there were undisclosed peaks observed on the surface of the gold nanoparticles, suggesting that the bioorganic phase had undergone prior crystallization. Considering that the diffraction peaks matched the standard database files of silver (JCPDS card No. 04-0783), it may be concluded that the synthesized AuNPs had a crystalline structure **(Fig:7).**

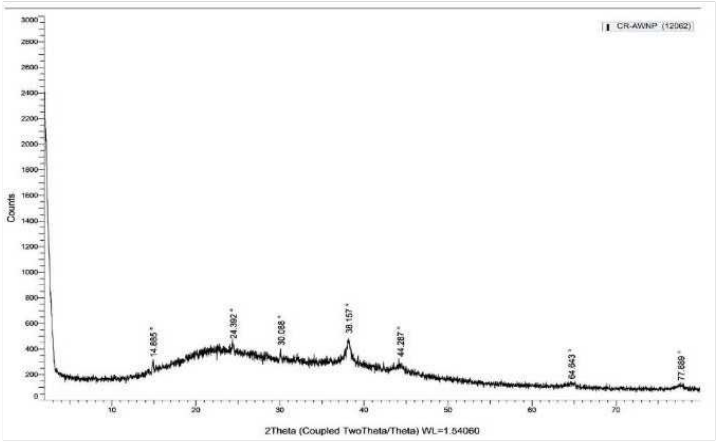

Fig : 7. XRD Spectra of CR-AuNPs

Characterization of Au-NPs by Zeta Potential

The characterization of Au-NPs derived from *C. rottleri* leaf extract using Zeta Potential Zeta potential provides an insight about the colloidal stability of nanoparticles. When it comes to nanoparticles, high degrees of stability are often associated with Zeta Potential values that are either larger than +25 mV or less than -25 mV.

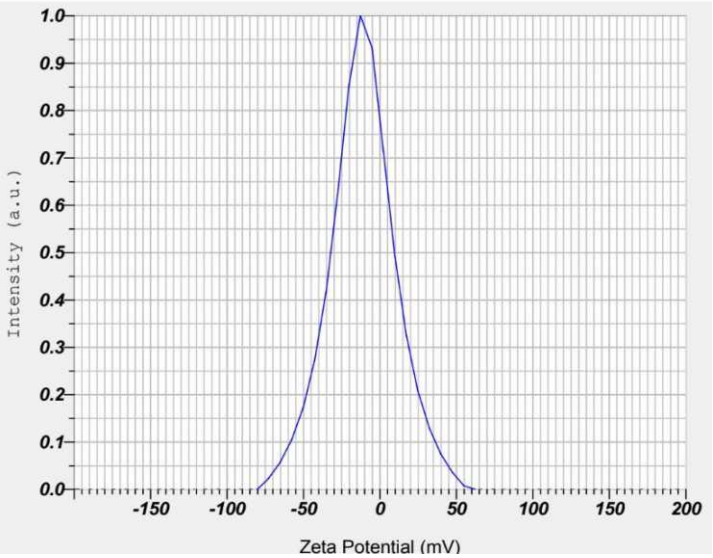

Fig:8. Zeta potential Spectra of CR AgNPs

Antioxidant activity

DPPH Free Radical Scavenging Activity of Ascorbic acid

The 1,1-diphenyl-2-picryl hydrazyl radical (DPPH) method was employed to evaluate the CR-AuNPs leaves' ability to scavenge free radicals. In 1mL of DPPH methanol solution (0.2 mM), differentiable chemical concentrations (10, 25, 50, 75, and 100µg/ml) were employed in this experiment. The optical density of the solution was then measured at 517 nm using the Hitachi-2010 spectrophotometer. The test sample results were compared to those of ascorbic acid (Vitamin C), a positive control, in order to calculate the percent inhibition of antioxidant activity.

The typical ascorbic acid's ability to scavenge free radicals with DPPH was concentration dependent. At high concentration levels, the activity gradually increased in parallel with the concentration. This was demonstrated by the results. However, the graph achieved a plateau state at high concentration. Ascorbic acid demonstrated the maximum percentage of inhibition at 83.62±0.785 in 100µg/mL, while the lowest concentration of activity was 18.53±0.162 in 10µg/mL, respectively (Table 2 & Fig:9).

Table:2. DPPH Free Radical Scavenging Activity of Ascorbic acid

Test Compound	Concentration (µg/mL)	% Inhibition
Ascorbic acid	10	18.53±0.162
	25	39.28±0.524
	50	51.16±0.579
	75	72.31±0.723
	100	83.62±0.785

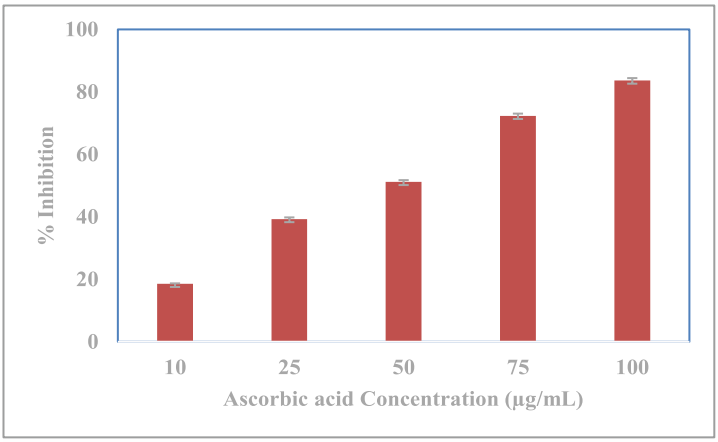

Fig: 9. DPPH Free Radical Scavenging Activity of Ascorbic acid

DPPH Free Radical Scavenging Activity of *C. rottleri*

The capacity of the CR - AuNPs scavenge free radicals was assessed using the method known as 1,1-diphenyl-2-picryl hydrazyl radical (DPPH). The results showed that the concentration had an effect on the percentage of inhibition brought on by *C. rottleri*. With an estimated value of 68.7±0.537, the maximum percentage of inhibition was observed at a dosage of 100 µg/mL. A dose of 50 µg/mL resulted in an inhibition percentage of 38.4±0.357, suggesting a moderate level of inhibition. The quantity of 10 µg/mL was found to produce the lowest percentage of inhibition (9.62±0.118). (Table 3 & Fig:10).

Table: 3. DPPH Free Radical Scavenging Activity of CR-AuNPs

Test Compound	Concentration (µg/mL)	% Inhibition
CR-AuNPs	10	9.62±0.118
	25	21.39±0.234
	50	38.4±0.357
	75	54.51±0.506
	100	68.7±0.537

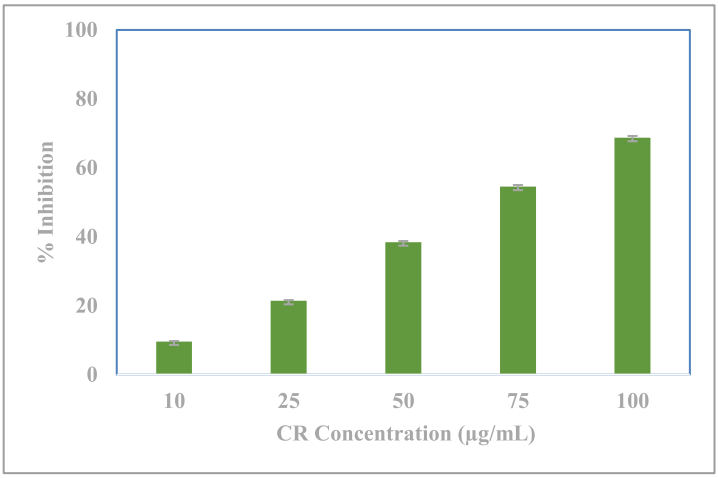

Fig: 10. DPPH Free Radical Scavenging Activity of CR-AuNPs

Hydrogen peroxide radical scavenging (H2O2) Assay of Ascorbic acid

The Ascorbic acid (standard) was used as the standard in the hydrogen peroxide radical scavenging assay (SA), and the concentrations of hydrogen peroxide (10, 25, 50, 75, and 100 µg/mL) were measured by spectrophotometer absorption at 230 nm. It was calculated what percentage of hydrogen peroxide was scavenged. An analysis of the H_2O_2 assay of ascorbic acid revealed that the percentage of inhibition is maximum at 100 µg/mL, with a value of 87.27±0.467, while the lowest percentage of inhibition is 19.52±0.225 at 10 µg/mL ((Table 4 & Fig:11).

Table:4.Hydrogen peroxide radical scavenging (H2O2) Assay of Ascorbic acid

Test Compound	Concentration (µg/mL)	% Inhibition
Ascorbic acid	10	19.52±0.225
	25	41.68±0.318
	50	62.93±0.364
	75	76.81±0.431
	100	87.27±0.467

Hydrogen peroxide radical scavenging (H_2O_2) Assay of *C. rottleri*

There was a concentration-dependent relationship between the scavenging activity of *C. rottleri* AuNPs on hydrogen peroxide, as shown in Figure(). The concentrations tested were 10, 25, 50, 75, and 100 µg/mL.

The CR -AuNPs shown a noteworthy ability to scavenge H_2O_2, with the lowest percentage of inhibition being 9.56±0.283 at a concentration of 10 µg/mL and the greatest percentage being 70.85±0.513 at a concentration of 100 µg/mL (Table 5 & Fig:12).

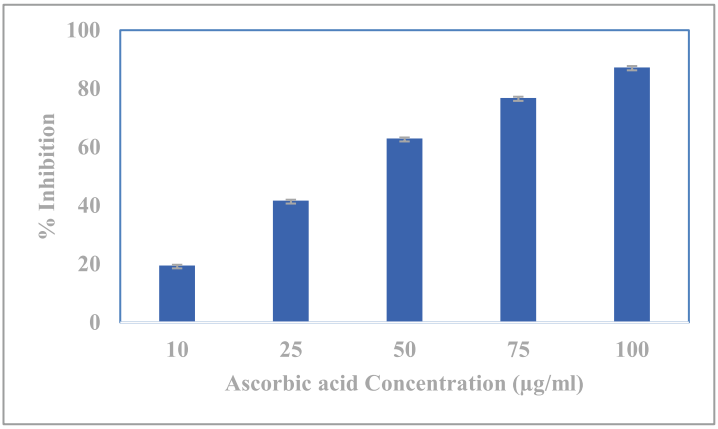

Fig: 11. Hydrogen peroxide radical scavenging (H2O2) Assay of Ascorbic acid

Table : 5. Hydrogen peroxide radical scavenging (H2O2) Assay of CR-AuNPs

Test Compound	Concentration (µg/mL)	% Inhibition
CR- AuNPs	10	9.56±0.283
	25	23.27±0.342
	50	41.64±0.372
	75	59.92±0.448
	100	70.85±0.513

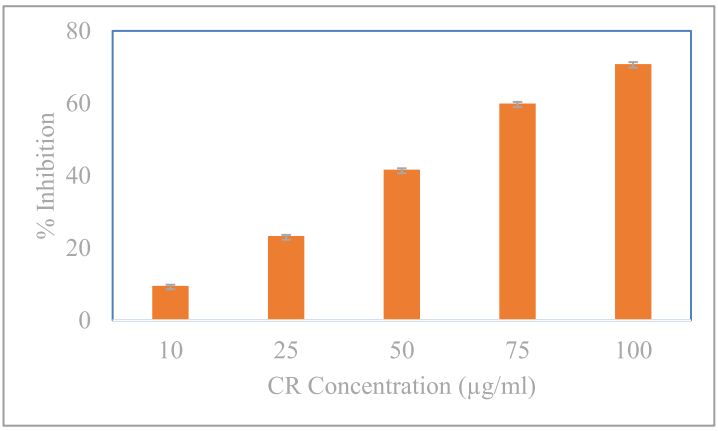

Fig: 12. Hydrogen peroxide radical scavenging (H2O2) Assay of CR-AuNPs

Anti-bacterial activity

The antibacterial properties of gold nanoparticles (AuNPs) derived from the C. *rottleri* plant leaves were investigated using the Agar well-diffusion method. Four concentrations (25, 50, 75, and 100 µg/µL) were tested, with ampicillin used as the standard antibiotic agent. The study focused on pathogenic strains, specifically *Staphylococcus aureus*, *E. coli*, *Streptococcus pneumonia*, and *Pseudomonas aeruginosa*. The assessment contrasted the effectiveness of CR-AuNPs, as shown in Table 6 and Figure 13 and 14, to that of ampicillin. The results revealed clear patterns in terms of bacterial strains and concentrations.

As an illustration, *Staphylococcus aureus* exhibited a growing area where bacterial growth was inhibited when exposed to ampicillin. The inhibition zone reached its highest point at 25 mm when the concentration of ampicillin was 100 µg. On the other hand, the CR-AuNPs demonstrated significant inhibition, particularly at lower concentrations. The maximum inhibition zone was observed at 12 mm when the concentration of CR-AuNPs was 75 µg, and at 14 mm when the concentration was 100 µg. In comparison, *E. Coli* exhibited inhibition ranging from 11 to 16 mm when treated with ampicillin at various concentrations. On the other hand, CR-AuNPs demonstrated low inhibition, measuring between 1.4 and 16 mm. *Streptococcus pneumoniae* also exhibited heightened vulnerability, as the areas of inhibition expanded from 1.2 to 17 mm at higher concentrations. Similarly, CR-AuNPs shown increasing susceptibility against *Pseudomonas aeruginosa*, with maximum inhibitory effects reaching a peak of 18 mm at a concentration of 100 µg (Table 6 & Fig:13&14).

To conclude, while Ampicillin consistently demonstrates inhibitory effects across bacterial strains, the efficacy of the CR-AuNPs varies, indicating potential as a source for antibacterial agents.

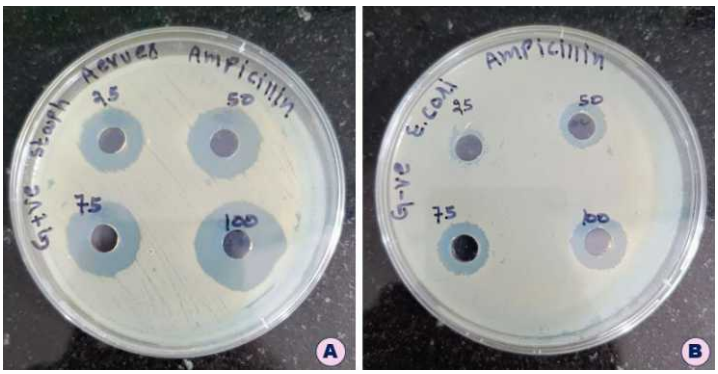

Fig: 13. Anti-bacterial activity of Standard Ampicillin (A) Staphylococcus aureus (B) E. coli

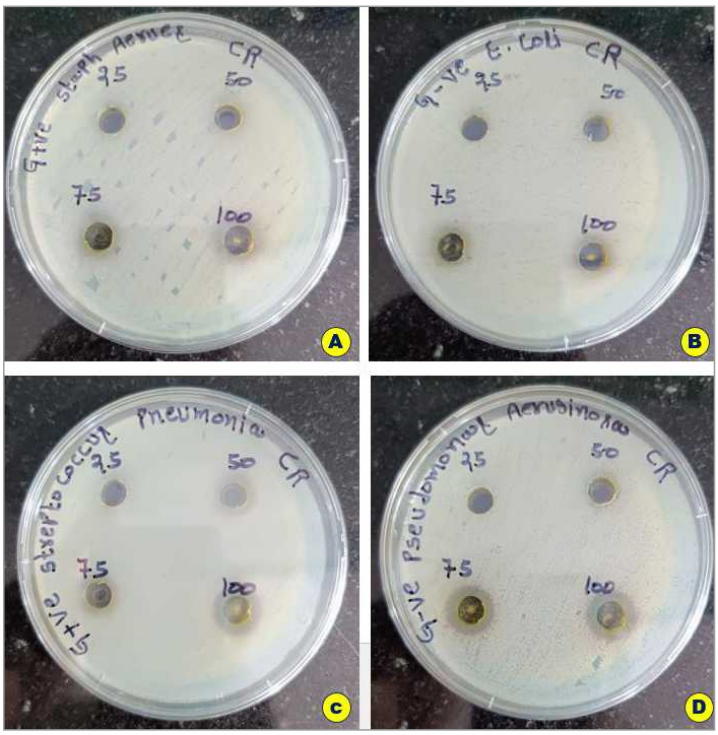

Fig: 14. Anti-Bacterial Activity of CR-AuNPs (A) S. aureus (B) E. coli (C) S. pneumonia (D) P. aeruginosa

Minimum Inhibitory Concentration (MIC) of CR-AuNPs

The Minimum Inhibitory Concentration (MIC) is defined as the lowest concentration of an antimicrobial agent that inhibits visible growth of a microorganism after overnight incubation. In this study, the MIC of C. rottleri-derived AuNPs was determined for bacterial species, including E. coli and Staphylococcus aureus, using ampicillin as the standard antibacterial agent. The assay was performed in nutrient broth with varying

concentrations of the test compounds, and the samples, along with the standard, were incubated overnight at 37°C. After 24 hours of treatment, the tubes were observed, and the results were recorded. The MIC results are detailed in Table 7 and illustrated in Figures 15 to 20.

Table 7 (pictures 15 and 16) displays the survival capacity of *Staphylococcus aureus* and *Escherichia coli* bacterial strains when exposed to different concentrations (µg/ml) of Ampicillin and CR-AuNPs. The resistance of *Staphylococcus aureus* to Ampicillin reduces as the concentration increases. The minimum inhibitory concentration (MIC) drops from 0.335 µg/ml at 5 µg/ml to 0.098 µg/mL at 200 µg/mL. However, the susceptibility of *Escherichia coli* to Ampicillin reduces as the concentrations increase. Specifically, the minimum inhibitory concentration (MIC) for *Escherichia coli* decreases from 0.295 µg/mL at a dose of 5 µg/mL to 0.114 µg/mL at a concentration of 200 µg/mL. Furthermore, the susceptibility levels of CR-AuNPs on *Escherichia coli* differ, with minimum inhibitory concentration (MIC) values ranging from 0.396 µg/ml at 5 µg/ml to 0.266 µg/ml at 200 µg/mL. Similar to *S. pneumoniae*, the sensitivity to CR-AuNPs diminishes as the concentration increases. The minimum inhibitory concentration (MIC) for *S. pneumoniae* is 0.406µg/mL at a concentration of 5 µg/mL, and 0.269µg/mL at a concentration of 200 µg/mL. In addition, *P. aeruginosa* displays a varied susceptibility pattern. The minimum inhibitory concentration (MIC) for *P. aeruginosa* is 0.397µg/mL at a concentration of 5 µg/mL, and 0.252µg/mL at a concentration of 200 µg/mL (Table :7 & Figures 15 to 20).

Table:6. Anti-Bacterial Activity of CR-AuNPs (A) S. aureus (B) E. coli (C) S. pneumonia (D) P. aeruginosa

Sr. No	Bacterial Strains	Ampicillin				CR-AuNPs			
		Concentration (µg/µL)/ Zone of Inhibition (mm)							
		25	50	75	100	25	50	75	100
1	*S. aureus*	16	20	22	25	0.8	10	12	14
2	*E. coli*	11	13	14	16	1.4	6	14	16
3	*S. pneumonia*					1.2	12	14	17
4	*P. aeruginosa*					0.6	12	16	18

Table:7. MIC activity of Ampicillin and CR-AuNPs

S. No	Bacteria	Concentration (µg/mL) Ampicillin						Concentration (µg/ml) CR-AuNPs					
		5	10	25	50	100	200	5	10	25	50	100	200
1.	*S. aureus*	0.335	0.304	0.256	0.253	0.194	0.098	0.392	0.386	0.383	0.365	0.294	0.257
2.	*E. coli*	0.295	0.283	0.276	0.285	0.206	0.114	0.396	0.389	0.392	0.363	0.324	0.266
3.	*S. pneumoniae*							0.406	0.388	0.383	0.361	0.314	0.269
4.	*P. aeruginosa*							0.397	0.384	0.389	0.357	0.306	0.252

1. Standard: Ampicillin *(Concentrations 5, 10, 25, 50 ,100 and 200µg/ml*

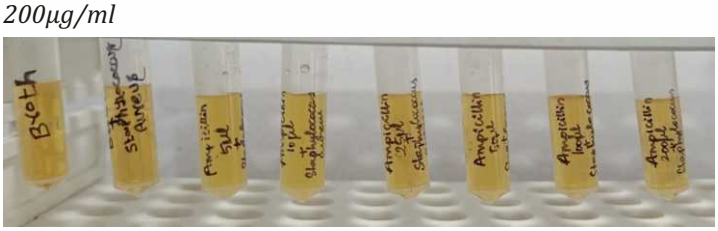

Fig:15. MIC activity of Ampicillin on S. aureus

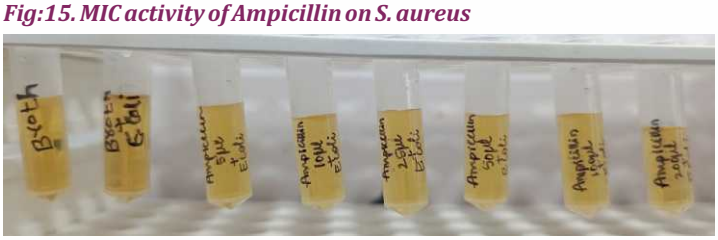

Fig :16. MIC activity of Ampicillin on E. coli

2. CR-AuNPs *(Concentrations 5, 10, 25, 50 ,100 and 200µg/mL)*

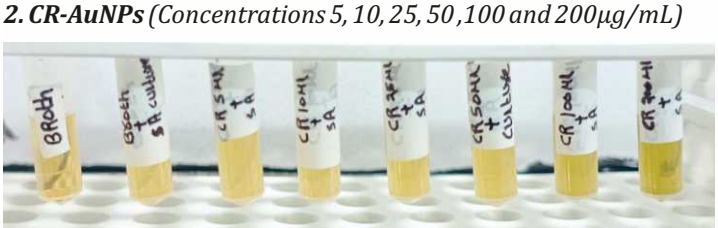

Fig :17. MIC activity of CR-AuNPs on S. aureus

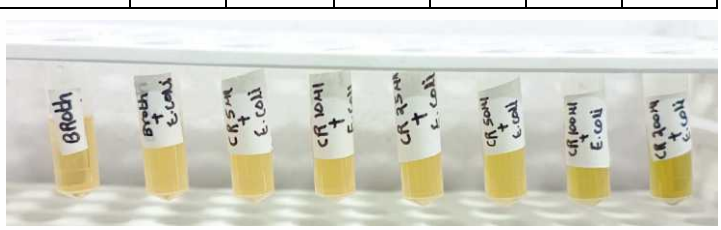

Fig :18. MIC activity of CR-AuNPs on E. coli

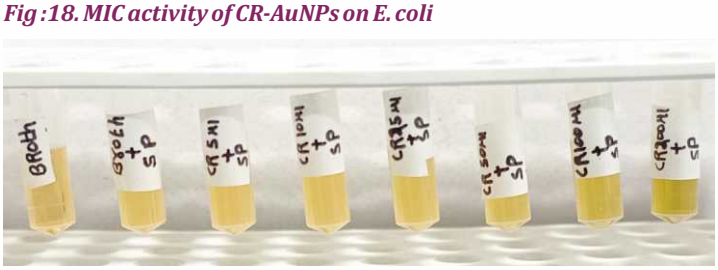

Fig :19. MIC activity of CR-AuNPs on S. pneumoniae

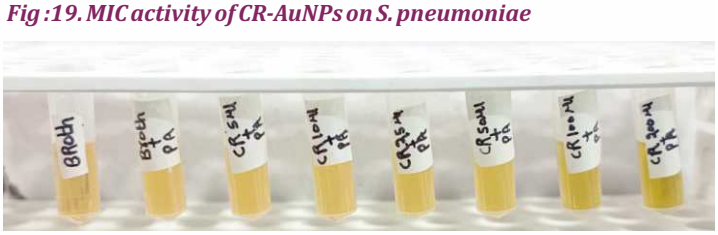

Fig:20. MIC activity of CR-AuNPs on P. aeruginosa

Antifungal activity

The antifungal activity of C. rottleri-derived AuNPs was assessed against fungal strains Candida albicans (MTCC 183) and Aspergillus niger (MTCC 281) using the well diffusion method on SDA culture plates. The plates were incubated at 37 ± 2°C for 48 hours to allow for fungal growth. After the incubation period, the plates were examined for zones of inhibition around the wells, and the diameters of these zones (in mm) were measured. Fluconazole was used as the standard antifungal agent for comparison. The fungal strains were obtained from the Microbial Type Culture Collection (MTCC) at the Institute of Microbial Technology (IMTECH), Chandigarh of India.

The table delineates the response of *C. albicans* and *A. niger strains* to Fluconazole alongside AuNPs, sourced from *C. rottleri* leaf. These responses were measured through respective zones of inhibition (mm) at different concentration levels (µg).

Fluconazole

Fig:21. Anti-fungal Activity of Fluconozole A. Candida albicans B. Aspergillus niger

Fluconazole is a drug used for antifungal purposes that shows varying levels of activity against different strains of *C. albicans* and *A. niger* as the concentration increases. The zones of inhibition for *A. niger* gradually increase from 12 mm at 25 µg to 25 mm at 100 µg, while the zones of inhibition for *C. albicans* gradually expand from 13 mm at 25 µg to 22 mm at 100 µg. This demonstrates a dose-dependent pattern and confirms its ability to suppress the growth of *C. albicans* and *A. niger* (Table: 8 and Fig:21

Table:8. Antifungal activity of Fluconazole

		Fluconazole Concentration (µg)/ Zone of Inhibition (mm)			
SNo	**Strain**	**25**	**50**	**75**	**100**
1	*Candida albicans*	13	16	18	22
2	*Aspergillus niger*	12	16	21	25

In contrast, the CR-AuNPs demonstrate a significant inhibitory impact on *Candida albicans* at lower dosages of 25 µg and 50 µg. However, when the quantities of 75 µg and 100 µg are increased, a significant zone of inhibition becomes apparent, measuring 17 mm and 19 mm respectively. The presence of *Aspergillus niger* was strongly inhibited by increasing concentrations of the substance. At a low concentration of 25 µg, a zone of inhibition measuring 12mm was seen, while the highest dose of 100 µg resulted in a substantial zone of inhibition measuring 23mm. This suggests that the CR-AuNPs may possess antifungal capabilities, albeit they are mostly noticeable at higher doses. This indicates that the CR-AuNPs may have stronger antifungal properties than fluconozole especially at higher concentrations (Table: 9 & Fig:22).

Table:9 Antifungal activity of CR-AuNPs

		CR-AuNPs Concentration (µg)/ Zone of Inhibition (mm)			
S. No	**Strain**	**25**	**50**	**75**	**100**
1	*Candida albicans*	11	14	17	19
2	*Aspergillus niger*	12	15	19	23

Anti-fungal Activity of CR-AuNPs

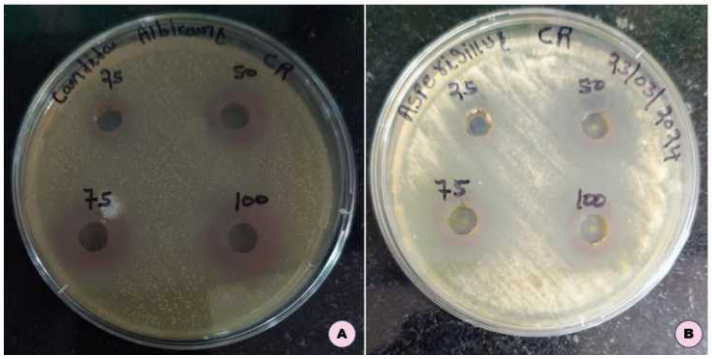

Fig:22. Anti-fungal activity of CR-AuNPs. A. C. albicans, B. A. niger

Disscussion

Chrozophora rottleri (Geiseler) Spreng., commonly known as "Suryavarti," is a member of the Euphorbiaceae family. This erect, hairy annual plant typically thrives in waste lands and flowers abundantly from January to April. It is native to various regions including India, Myanmar, Thailand, the Andaman Islands, and Central Java, Malesia. Traditionally, C. rottleri has been used in indigenous medicine for treating a range of ailments.

In Saudi Arabia, Pakistan, and India, it is utilized for conditions such as jaundice and blood purification. In India and Sudan, powdered stems or whole plants are applied to wounds to promote healing. In Nepal, the fruit juice serves as a remedy for coughs and colds, while the leaves act as a purifying agent, and the seeds function as a laxative. Additionally, the fruit produces a purplish-blue dye used in East Africa for coloring mats. The leaves are also known for their efficacy in treating skin diseases and are used as a depurative agent. The synthesis and characterization of nanoparticles represent a rapidly advancing area in science and technology [57]. Utilizing plant materials for nanoparticle synthesis is particularly advantageous due to the simplicity of the process and the absence of complex procedures [59].

In the present investigation, *C. rottleri* leaf extract was effectively used to produce gold nanoparticles. Color changes were used for observing the interaction between *C. rottleri* extract and gold ions. It was noticed that the 1 mM $HAuCl_4 \cdot 3H_2O$ solution turned wine red within a minute of the addition of a *C. rottleri* leaf extract solution. This color shift implies the solution is synthetic AuNPs. The solution started out golden yellow. The development of colloidal gold nanoparticles in substrates can be determined by the presence of ruddiness in color.

The formation of gold nanoparticles with colloidal structure in the natural environment can be detected by their formation of wine-red color. Because the metal nanoparticles' surface plasmon vibrations are excited, creating a surface plasmon resonance band with a center of around 536 nm, gold nanoparticles appear wine red in aqueous conditions [59].

In this investigation, CR-AuNPs exhibited wine-red hues and a high peak plasmon band that was visible in the UV-Vis spectra between 580 and 620 nm. The sharpness of the absorption peak was shown to be correlated with the extract volume ratio, meaning that a larger ratio corresponded to a sharper peak.This result is consistent with previously published values [60]. The biomolecules were categorized using FTIR spectroscopy based on their functional groups, which helped to stabilize and reduce the produced AuNPs [61-62]. Several functional groups were found in the current study's FTIR analyses of CR-AuNPs, including 692.47, which is associated with the =C-H Alkane, and 1631.83 and 1641.78, which are associated with the C-O Alkenyl. The C=CH Aliphatic compounds are shown by the peak 1901.88; the C=C Alkynes are represented by the peak 2931.90; the C=N-H amides and N-H amine and amides are shown by the peak 3522.13.

According to [63-64] surface morphology microscopy (SEM) is a method of surface imaging that can distinguish between different particle sizes, size distributions, nanomaterial forms, and the surface morphology of manufactured particles at the micro- and nanoscales. High-resolution SEMs of today can identify nanoparticles with morphologies less than 10 nm. [65-68] describe how backscattered electrons, or BSEs, are used in this imaging technique. The round shape with a diameter ranging from 132 to 146 nm was revealed by the current SEM examination of CR-AuNPs.

According to the XRD examination, CR-AuNPs are crystalline. A series of Bragg reflection peaks were seen at 2 θ value, corresponding to (111), (200), (220), and (311) facets crystallographic planes of face-centered cubic The diffraction peaks (JCPDS card No. 04 0783) matched the standard database files of gold.

Zeta potential analysis was used to assess the stability and surface charge of the synthesized CR-AuNPs [64]. AuNPs with a zeta potential above +25 mV or below -25 mV generally exhibit high stability. Positive values suggest potential aggregation, while negative values indicate strong surface charges that prevent agglomeration and ensure stability.

The antioxidant activity of Chrozophora rottleri-derived gold nanoparticles (CR-AuNPs) was evaluated using the DPPH method, which measures the ability to eliminate free radicals. This activity was compared to that of ascorbic acid, a standard antioxidant. At a concentration of 100 µg/mL, ascorbic acid exhibited the highest percentage of free radical inhibition at 83.62±0.785%. Conversely, at a lower concentration of 10 µg/mL, ascorbic acid's inhibition activity significantly decreased to 18.53±0.162%. For CR-AuNPs, the concentration also played a crucial role in their antioxidant efficacy. At 100 µg/mL, CR-AuNPs achieved their highest inhibition percentage at 68.7±0.537%, demonstrating a strong antioxidant capacity, albeit lower than that of ascorbic acid at the same concentration. At 50 µg/mL, the inhibition percentage was moderate, measured at 38.4±0.357%, which indicates a significant reduction in free radical scavenging ability compared to the highest concentration. At the lowest tested concentration of 10 µg/mL, CR-AuNPs displayed the least inhibition activity at 9.62±0.118%.These results indicate that both ascorbic acid and CR-AuNPs show a concentration-dependent antioxidant activity, with higher concentrations leading to greater free radical inhibition. However, ascorbic acid consistently outperforms CR-AuNPs at equivalent concentrations.

The H_2O_2 assay revealed that ascorbic acid exhibited its highest inhibition percentage (87.27±0.467%) at 100 µg/mL, while the inhibition dropped to its lowest (19.52±0.225%) at 10 µg/mL. CR-AuNPs also showed a concentration-dependent inhibition of H_2O_2. At 100 µg/mL, CR-AuNPs reached their peak inhibition percentage at 70.85±0.513%, while the lowest inhibition percentage was 9.56±0.283% at 10 µg/mL. These results highlight that both ascorbic acid and CR-AuNPs have significant antioxidant activities that increase with concentration, with ascorbic acid consistently demonstrating higher inhibition than CR-AuNPs at the same concentrations.

In the comparative study of antibacterial activities, both ampicillin and CR-AuNPs exhibited varying degrees of effectiveness against different bacterial strains, in different ways: At 100 µg concentration, ampicillin demonstrated a significant antibacterial effect against *Staphylococcus aureus*, exhibiting a 25 mm inhibition zone. It was demonstrated that CR-AuNPs significantly inhibited at lower concentrations, exhibiting an inhibition zone of 12 mm at 75 µg and 14 mm at 100 µg. Ampicillin had modest antibacterial activity against *E. coli*, with inhibition zones ranging from 11 to 16 mm across concentrations. Zones of *E. Coli* inhibition from CR-AuNPs ranged from 1.4 to 16 mm, and they were moderate. The concentration of ampicillin caused the inhibition zones of *Streptococcus pneumoniae* to grow from 1.2 mm to 17 mm, showing enhanced susceptibility. When exposed to 100 µg of antibacterial activity, CR-AuNPs showed 18 mm inhibitory zones. Using 100 µg of *Pseudomonas aeruginosa*: CR-AuNPs, there was a maximum inhibition of 18 mm, indicating substantial antibacterial activity. Overall, CR-AuNPs showed promising antibacterial activity, particularly at lower concentrations, against multiple bacterial strains.

A study was conducted on bacterial species like *E. coli* and *S. aureus* using ampicillin as a standard antibacterial. Results showed that resistance to Ampicillin decreases as concentration increases, while susceptibility to *E. coli* decreases. The susceptibility levels of CR-AuNPs on *E.coli* differ, with MIC values ranging from 0.396 to 0.266 µg/ml. Similar to *S. pneumoniae*, sensitivity to CR-AuNPs diminishes as concentration increases.

The study examined the antifungal activity of fluconazole (standard) and CR-AuNPs against *Candida albicans* and *Aspergillus niger*. For fluconazole, the inhibition zones for *C. albicans* increased from 13 mm at 25 µg to 22 mm at 100 µg, and for *A. niger*, they expanded from 12 mm at 25 µg to 25 mm at 100 µg. This dose-dependent pattern demonstrates fluconazole's efficacy in inhibiting the growth of both *C. albicans* and *A. niger*. Regarding CR-AuNPs, significant inhibition was observed at lower concentrations for *C. albicans*, with inhibition zones of 17 mm at 75 µg and 19 mm at 100 µg. For *A. niger*, the inhibition zones increased from 12 mm at 25 µg to 23 mm at 100 µg. These findings suggest that at higher concentrations, CR-AuNPs might be more effective than ampicillin against these fungal strains.

Conclusions

This work is the first to describe the synthesis of AuNPs from *C. rottleri* leaves. A leaf extract of *C. rottleri* (Euphorbiaceae) is capable of producing gold nanoparticles (AuNPs), which have been demonstrated recently to have antibacterial and anti-oxidant properties. This study offers a more environmentally friendly approach to the synthesis of Phyto-mediated gold nanoparticles.

Comparing this synthetic approach to the chemical method, it is less noxious and more environmentally friendly because it doesn't require any reductant or surfactant. It might be a source of encouragement for future studies as workable agents for use in pharmaceutical and medical applications. Our study will be concentrating on synthesizing various kinds of green nanoparticles in the future to create applications in the pharmaceutical, medicinal, environmental, aquaculture, and agricultural sectors. The findings of this study provide guidance for future research in the production of green nanoparticles in the environmental and biological sectors.

Acknowledgments

The authors would like to thank the Head, Department of Botany, Osmania University, Hyderabad, Telangana for their invaluable support that made the authors work possible.

References

1. Ahmad, M.; Nirmal, N.P.; Danish, M.; Chuprom, J.; Jafarzedeh, S. (2016). Characterisation of composite films fabricated from collagen/chitosan and collagen/soy protein isolate for food packaging applications. RSC Adv. 6, 82191–82204.

2. Ahmad, N.; Bhatnagar, S.; Saxena, R.; Iqbal, D.; Ghosh, A.K.; Dutta, R. (2017). Biosynthesis and characterization of gold nanoparticles: Kinetics, in vitro and in vivo study. Mater. Sci. Eng. C. 78, 553–564.

3. Ahmed, S.; Annu; Ikram, S.; Yudha, S.S. (2016). Biosynthesis of gold nanoparticles: A green approach. J. Photochem. Photobiol. B 2016, 161, 141–153.

4. Ahmed, W., Azmat, R., Mehmood, A., Qayyum, A., Ahmed, R., Khan, S.U., Liaquat, M., Naz, S. and Ahmad, S. (2021). The analysis of new higher operative bioactive compounds and chemical functional group from herbal plants through UF-HPLC-DAD and Fourier transform infrared spectroscopy methods and their biological activity with antioxidant potential process as future green chemical assay. Arabian Journal of Chemistry, 14(2), p.102935.

5. Ahn, E.-Y.; Hwang, S.J.; Choi, M.J.; Cho, S.; Lee, H.-J.; Park, Y. (2018). Upcycling of jellyfish (Nemopilema nomurai) sea wastes as highly valuable reducing agents for green synthesis of gold nanoparticlesand their antitumor and anti-inflammatory activity. Artif. Cells Nanomed. Biotechnol., 46, 1127–1136.

6. Aili M, Zhou K, Zhan J, Zheng H, Luo F .(2023). Anti-inflammatory role of gold nanoparticles in the prevention and treatment of Alzheimer's disease. Journal of Materials Chemistry B: 8605–8621. https://doi.org/10.1039/d3tb01023f.

7. Ajay Kumar Meena and M M Rao. (2010). Folk herbal medicines used by the Meena community in Rajasthan. Asian Journal of Traditional Medicines, 5 (1), 19-31.

8. Alex S, Tiwari A. (2015). Functionalized gold nanoparticles: Synthesis, properties and applications-A review. Journal of Nanoscience and Nanotechnology 15: 1869–1894. https://doi.org/10.1166/jnn.2015.9718.

9. Amina, S.J.; Guo, B. A Review on the Synthesis and Functionalization of Gold Nanoparticles as a Drug Delivery Vehicle. Int. J. Nanomed. (2020). 15, 9823–9857.

10. Anand, K.; Tiloke, C.; Pragalathan, N.; Chuturgoon, A.A. (2012). huturgoon Phytonanotherapy for management of diabetes using green synthesis nanoparticles. J. Photochem. Photobiol. B 2017, 173, 626–639.

11. Andleeb, A.; Andleeb, A.; Asghar, S.; Zaman, G.; Tariq, M.; Mehmood, A.; Nadeem, M.; Hano, C.; Lorenzo, J.M.; Abbasi, B.H. (2021). A Systematic Review of Biosynthesized Metallic Nanoparticles as a Promising Anti-Cancer-Strategy. Cancers, 13, 2818.

12. Arafa, M.G., El-Kased, R.F. M.M. (2018). Elmazar Thermoresponsive gels containing gold nanoparticles as smart antibacterial and wound healing agents. Sci Rep, 8 (1) pp. 1-6.

13. Arokiyaraj S., Saravanan M., Badathala V. (2015). Green synthesis of silver nanoparticles using aqueous extract of Taraxacum officinale and its antimicrobial activity. South Indian J. Biol. Sci., 2, pp. 115-118.

Asia Pacific Medicinal Plant Database. (2010).

14. Bakur, A.; Niu, Y.; Kuang, H.; Chen, Q. (2019). Synthesis of Gold Nanoparticles Derived from Mannosylerythritol Lipid and Evaluation of Their Bioactivities. AMB Express, 9, 62.

15. Baliyan S, Mukherjee R, Priyadarshini A, Vibhuti A, Gupta A, Pandey RP, Chang CM. (2022). Determination of Antioxidants by DPPH Radical Scavenging Activity and Quantitative Phytochemical Analysis of Ficus religiosa. Molecules. Feb 16;27(4):1326. doi: 10.3390/molecules27041326. PMID: 35209118; PMCID: PMC8878429.

16. Basavegowda, N.; Idhayadhulla. (2014). A.; Lee, Y.R. Tyrosinase Inhibitory Activity of Silver Nanoparticles Treated with Hovenia dulcis Fruit Extract: An in Vitro Study. Mater. Lett. 2014, 129, 28–30.

17. Bhandari R, Pant D, Kathayat KS, Bhattarai R, Barakoti H, Pandey J, Jamarkatel-Pandit N. (2023). Preliminary Study on the Antibacterial Activities and Antibacterial Guided Fractionation of Some Common Medicinal Plants Practices in Itum Bahal, Kathmandu Valley of Nepal. ScientificWorldJournal. Sep 21; 2023:7398866. doi: 10.1155/2023/7398866. PMID: 37780640; PMCID: PMC10539093.

18. Chen R, Chen F, Sun M, Zhang R, Wu S, Meng C. (2022). Controllable synthesis and antioxidant activity of gold nanoparticles using chlorogenic acid. Inorganic and Nano-Metal Chemistry 52: 1345–1351. https://doi.org/10.1080/24701556.2021.1952242.

19. Connor, O, Sexton, D. J., St, R B. A.,., Smart, C., Eds.; Springer Berlin Heidelberg, (2003). Surface Analysis Methods in Materials Science. In Springer Series in Surface Sciences;

20. Connor, O, Sexton, D. J., St, R B. A.,., Smart, C., Eds.; Springer Berlin Heidelberg, (2003). Surface Analysis Methods in Materials Science. In Springer Series in Surface Sciences;

21. Ebrahimzadeh, M.A. and Bahramian, F. (2009). Antioxidant Activity of Crataegus pentaegyna Subsp. elburensis Fruits Extracts Used in Traditional Medicine in Iran. Pakistan Journal of Biological Sciences, 12: 413-419.

22. Filip, G.A.; Moldovan, B.; Baldea, I.; Olteanu, D.; Suharoschi, R.; Decea, N.; Cismaru, C.M.; Gal, E.; Cenariu, M.; Clichici, S.; et al. (2019). UV-light mediated green synthesis of silver and gold nanoparticlesusing Cornelian cherry fruit extract and their comparative effects in experimental inflammation. J. Photochem. Photobiol. B, 191, 26–37.

23. Fissan, H.; Ristig, S.; Kaminski, H.; Asbach, C.; Epple, M. (2014). Comparison of Different Characterization Methods for Nanoparticle Dispersions before and after Aerosolization. Anal. Methods 2014, 6,7324–7334.

24. Francis S, Siby Joseph, Ebey P. Koshy and Beena Mathew. (2017). Green synthesis and characterization of gold and silver nanoparticles using Mussaenda glabrata leaf extract and their environmental applications to dye degradation. Environ. Sci. Pollut. Res. 24, 17347–17357. https://doi.org/10.1007/s11356 017-9329-2.

25. Govindappa M, Hemashekhar B, Arthikala MK, Rai VR, Ramachandra YL. (2018). Characterization, antibacterial, antioxidant, antidiabetic, anti-inflammatory and antityrosinase activity of green synthesized silver nanoparticles using Calophyllum tomentosum leaves extract. Results Phys, 9:400–408.

26. Hammami I, Alabdallah NM, jomaa A Al, kamoun M .(2021). Gold nanoparticles: Synthesis properties and applications. Journal of King Saud University - Science 33(7): 101560. https://doi.org/10.1016/j.jksus.2021.101560.

27. Huang X., El-Sayed I.H., Qian W., El-Sayed M.A. (2006). Cancer cell imaging and photothermal therapy in the near-infrared region by using gold nanorods.J. Am. Chem. Soc., 128 pp. 2115-2120.

28. Italiano, F.; Agostiano, A.; Belviso, B.D.; Caliandro, R.; Carrozzini, B.; Comparelli, R.; Melillo, M.T.; Mesto, E.; Tempestae, G.; Trotta, M. (2018). Interaction between the photosynthetic anoxygenic microorganism Rhodobacter sphaeroides and soluble gold compounds. From toxicity to gold nanoparticle synthesis. Colloids Surf. B , 172, 362–371.

29. Ju-Nam, Y.; Led, J.R. (2008). Manufactured Nanoparticles: An Overview of Their Chemistry, Inclination, and Potential Implication. Sci. Total Environ., 400, 396–4141.

30. Kalimuthu Kalishwaralal, Subhaschandrabose Jeyabharathi, Krishnan Sundar and Azhaguchamy Muthukumaran. (2014). A novel one-pot green synthesis of selenium nanoparticles and evaluation of its toxicity in zebrafi sh embryos. Artificial Cells, Nanomedicine and Biotechnology 1–7. https://doi.org/10.3109/21691401.2014.962744.

31. Kalimuthu, K., Cha, B.S., Kim, S., Park, K.S.J.M.J. (2020). Eco-friendly synthesis and biomedical applications of gold nanoparticles: a review. 152:104296.

32. Kar Xin Lee K, Thomas J. (2020). Recent developments in the facile biosynthesis of gold nanoparticles (AuNPs) and their biomedical applications. Int J Nanomed 15:275–300. https:// doi. org/ 10. 2147/ IJN. S2337 89.

33. Karthik, R.; Govindasamy, M.; Chen, S.-M.; Mani, V.; Lou, B.-S.; Devasenathipathy, R.; Hou, Y.-S.; Elangovan, A. (2016). Green synthesized gold nanoparticles decorated graphene oxide for sensitive determination of chloramphenicol in milk, powdered milk, honey and eye drops. J. Colloid Interface Sci. 475, 46–56.

34. Karuppiah, C.; Palanisamy, S.; Chen, S.-M.; Emmanuel, R.; Muthupandi, K.; Prakash, P. (2015). Green synthesis of gold nanoparticles and its application for the trace level determination of painter's colic. RSC Adv. 5, 16284–16291.

35. Khan, S.; Bakht, J.; Syed, F. (2018). Green synthesis of gold nanoparticles using acer pentapomicum leaves extract its characterization, antibacterial, antifungal and antioxidant bioassay. Dig. J. Nanomater. Biostruct., 13, 579–589.

36. Khare C.P. (2007). Indian Medicinal Plants: An Illustrated Dictionary. Springer.

37. Khoshnamvand, M.; Ashtiani, S.; Huo, C.; Saeb, S.P.; Liu, J. (2019). Use of Alcea rosea leaf extract for biomimetic synthesis of gold nanoparticles with innate free radical scavenging and catalytic activities. J. Mol. Struct. 1179, 749–755.

38. Kumar, H., Dhalaria, R., Guleria, S., Cimler, R., Sharma, R., Siddiqui, S. A., ... & Kuča, K. (2023). Anti-oxidant potential of plants and probiotic spp. in alleviating oxidative stress induced by H2O2. Biomedicine & Pharmacotherapy, 165, 115022.

39. Kumar, K.P.; Paul, W.; Sharma, C.P. (2011). Green synthesis of gold nanoparticles with Zingiber officinale extract: Characterization and blood compatibility. Process Biochem. 2011, 46, 2007–2013.

40. Kumar, P.V.; Kala, S.M.J.; Prakash, K.S. (2019). Green synthesis of gold nanoparticles using Croton Caudatus Geisel leaf extract and their biological studies. Mater. Lett., 236, 19–22.

41. Kumar, R. (2016). Anticancer Activity of Eco-Friendly Au Nanoparticles against Lung and Liver Cancer Cells. J. Genet. Eng. Biotechnol. 2016, 14, 195–202.

42. L.H. Fu, J. Yang, J.F. Zhu, M.G. Ma. (2017). Synthesis of gold nanoparticles and their applications in drug delivery Metal nanoparticles in pharma, Springer, Cham pp. 155-191.

43. Li X, Ni T, Xu R .(2023b). Study on the preparation of novel flavonol-gold nanoparticles antioxidants and the mechanism of protein corona formation. Journal of Molecular Structure 1294: 136413. https://doi.org/10.1016/j.molstruc.2023.13641.

44. Li, L.; Zhang, Z.J. (2016). Biosynthesis of Gold Nanoparticles Using Green Alga Pithophora oedogonia with Their Electrochemical Performance for Determining Carbendazim in Soil. Int. J. Electrochem. Sci., 11, 4550–4559

45. Meena, J. Gupta, A. Ahuja, R. Panda, A.K. Bhaskar, S. (2020). Inorganic particles for delivering natural products. Sustainable Agric. Rev., 44 pp. 205-241.

46. Mikhailova, E.O. (2021). Gold Nanoparticles: Biosynthesis and Potential of Biomedical Application. J. Funct. Biomater. 12, 70.

47. Mohamed, E. A. A., Muddathir, A. M., & Osman, M. A. (2020). Antimicrobial activity, phytochemical screening of crude extracts, and essential oils constituents of two Pulicaria spp. growing in Sudan. Scientific Reports,10:1, 10(1), 1–8.

48. Mukherjee, S.; Sau, S.; Madhuri, D.; Bollu, V.S.; Madhusudana, K.; Sreedhar, B.; Banerjee, R.; Patra, C.R. (2016). Green synthesis and characterization of monodispersed gold nanoparticles: Toxicity study, delivery of doxorubicin and its biodistribution in mouse model. J. Biomed. Nanotechnol. 12, 165–181.

49. Narmada T, RamyaDevi R, Sivaraman, Sand H, Sekar Babu. (2012). "Antioxidant activity of Chrozophora rottleri". Research Journal of Pharmaceutical, Biological and Chemical Sciences, vol.3,no.1,pp.593-596.

50. Nirmal, N.P.; Mereddy, R.; Li, L.; Sultanbawa, Y. Formulation. (2018). characterisation and antibacterial activity of lemon myrtle and anise myrtle essential oil in water nanoemulsion. Food Chem., 254, 1–7.

51. Pakkirisamy, M Suresh Kumar Kalakandan and Karthikeyen Ravichandran. (2017). Phytochemical screening, GC-MS, FT-IR analysis of methanolic extract of Curcuma caesia Roxb (Black Turmeric). Phcogj.Com, 9(6):952-956.

52. Patel, J.R. Gohil. D.T. (2017). "Anti-microbial activity of leaf extracts of Peltoporumv pterocarpum (DC)an invitro study". Life Sciences Leaflets, vol.90, no.1, pp.0976-1098,.

53. Perveen, K.; Husain, F.M.; Qais, F.A.; Khan, A.; Razak, S.; Afsar, T.; Alam, P.; Almajwal, A.M.; Abulmeaty, M.M.A. (2021). Microwave-Assisted Rapid Green Synthesis of Gold Nanoparticles Using Seed Extract of Trachyspermum ammi: ROS Mediated Biofilm Inhibition and Anticancer Activity. Biomolecules, 11, 197.

54. Rasmussen MK, Pedersen JN, Marie R. (2020). Size and surface charge characterization of nanoparticles with a salt gradient. Nat Commun 11:2337

55. Roopan, S.M. Priya, D.D., Shanavas, S., Acevedo, R., Al-Dhabi, N.A., Arasu. M.V., . (2019). CuO/C nanocomposite: Synthesis and optimization using sucrose as carbon source and its antifungal activity. Mater. Sci. Eng., C, 101 pp. 404-414.

56. Ruch, R.J. Chung, S.U. Klaunig, J.E. (1984). Spin trapping of superoxide and hydroxyl radicals Methods Enzymol., 105 pp. 198-209.

57. Safaepaser, M.; Shahverdi, A.R.; Shahverdi, H.R.; Khorramizadeh, M.R.; Gohari, A.R. (2009). Green Synthesis of Small Ag Nanoparticles Using Geraniol and Its Cytotoxicity against Fibrosarcomawehi 164. Avicenna J. Med. Biotechnol. 1, 111–115.

58. Sakthipriyadarsini, S., & Kumar, P. R. (2022). Evaluation of Hydrogen peroxide Scavenging and Antibacterial activity of successive extracts of Luisia tenuifolia Blume against skin and wound infections. Research Journal of Pharmacy and Technology, 15(10), 4565-4569.

59. Sathishkumar, P.; Gu, F.L.; Zhan, Q.; Palvannan, T.; Yusof, A.R.M. (2018). Flavonoids mediated 'Green' nanomaterials: A novel nanomedicine system to treat various diseases—Current trends and future perspective. Mater. Lett. , 210, 26–30.

60. Sevieri, M.; Silva, F.; Bonizzi, A.; Sitia, L.; Truffi, M.; Mazzucchelli, S.; Corsi, F.(2020). Indocyanine Green Nanoparticles: Are They Compelling for Cancer Treatment? Front. Chem., 8, 535.

61. Sharifi-Rad M, Kishore Mohanta Y, Pohl P, Nayak D, Messaoudi M .(2023). Facile phytosynthesis of gold nanoparticles using Nepeta bodeana Bunge: Evaluation of its therapeutics and potential catalytic activities. Journal of Photochemistry and Photobiology A: Chemistry 446: 115150. https://doi.org/10.1016/j.jphotochem.2023.115150.

62. Sharma, N.; Bhatt, G.; Kothiyal, P. (2015). Gold Nanoparticles synthesis, properties, and forthcoming applications: A review. Indian J. Pharm. Biol. Res. 2015, 3, 13–27.

63. Signati, L.; Allevi, R.; Piccotti, F.; Albasini, S.; Villani, L.; Sevieri, M.; Bonizzi, A.; Corsi, F.; Mazzucchelli, S. (2021). Ultrastructural analysis of breast cancer patient-derived organoids. Cancer Cell Int., 21, 423.

64. Sumithira S, Amsath, A, Govindarajan, M, and Muthukumaran U. (2013). "Mosquito Larvicidal effect of Chrozophora rottleri against Anopheles stephensi, Aedes Aegypti and Culex Quinque fasciatus (Diptera:Culicidae)".International Journal current Biochemistry and Biotechnology, vol.2,no. 1,pp.001-005.